Civil and Sustainable Urban Engineering

Research Article
Volume 3(1), 2023, 81-94
https://doi.org/10.53623/csue.v3i1.242

Development of Cement Stabilised Compressed Blocks Using Coal Bottom Ash: Influence of the Grain Size on Mechanical and Physical Properties of Blocks

Jacques Rémy Minane[1,2,*], Abdou Lawane[2], Jeremie Madjadoumbaye[1], Raffaele Vinai[3], Brice Zagré[2]

[1]Department of Civil Engineering, National Advanced School of Engineering of Yaounde (Polytechnic), University of Yaounde I, P.O. Box 8390 Yaounde, Cameroon
[2]International Institute of Water and Environment Engineering (2iE), Eco-Materials and Sustainable Habitat Laboratory (LEMHaD), Rue de la Science, 01 BP 194 Ouagadougou 01, Burkina Faso
[3]Department of Engineering, University of Exeter, Harrison Building, North Park Road, Exeter EX4 4QF, United Kingdom

*Correspondence: remy.minane@univ-yaounde1.cm

SUBMITTED: 7 April 2023; REVISED: 16 May 2023; ACCEPTED: 19 May 2023

ABSTRACT: This study investigated the physical and mechanical properties of cement-stabilized compressed blocks manufactured with coal bottom ash sourced from a power plant in Niger. Three different grain sizes were used for the production of compressed blocks with a hand-operated press. Thermal, hydric, mechanical, and fire resistance properties were assessed on the samples. It was found that the use of finer bottom ash resulted in lighter blocks with a density of about 1.02 mg/m^3 and thermal conductivity in the range of 0.27 – 0.41 W/m·K. The size of the bottom ash used for the production of blocks did not significantly affect the value of mechanical strength. The exposure of blocks to temperatures of 200°C and 400°C did not reduce the strength of the samples. Neat bottom ash blocks can offer better thermal properties than typical building materials and provide acceptable mechanical strength.

KEYWORDS: Coal bottom ash; compressed block; waste recycling; low carbon building materials

1. Introduction

The sustainable management of waste produced worldwide poses an extraordinary challenge for the 21st century. This challenge extends beyond environmental concerns, as the volume of waste continues to increase, affecting trade and geopolitics. According to a World Bank report [1], the world produces 2.01 billion tonnes of waste annually, with 33% of it not being properly managed. This rate is even higher in Southern countries, leading to environmental problems such as soil and water pollution, as well as threats to biodiversity. Additionally, social and health issues arise, including toxic fumes from uncontrolled waste burning and the collapse of illegal landfills. The energy and construction sectors are major contributors to waste production [2], often in the form of granular waste. Recycling such waste presents a significant business opportunity, with an estimated potential market value of 175 billion euros worldwide [3].

The recycling of granular waste in the construction sector has gained interest within the framework of a circular economy approach. The aim is twofold: to reduce the use of non-renewable natural resources and to limit waste landfill. Industrial activities in emerging countries, such as mineral coal mining, have both positive and negative impacts. While they provide economic development opportunities and job creation, concerns arise regarding potential negative repercussions on local social fabric and the environment. Despite ongoing discussions about limiting its use for energy production, coal still holds a significant share in the global energy industry. According to the World Coal Association [4], mineral coal mining accounts for 38% of the world's electricity production and 71% of steel production. Although coal is responsible for 35% of CO_2 emissions [5], its availability and cost make it a preferred energy source. Therefore, coal will continue to play an important role in electricity production for several decades, at least in certain regions. The combustion of mineral coal generates fly ash (FA), bottom ash (BA), and other coal combustion residues. Previous studies have successfully demonstrated the utilization of these residues in various applications, including the manufacturing of cement-stabilized bricks [6, 7], ceramics [8], substitute for natural sand in concrete production [9–11], and cement production [12].

Niger is rich in coal resources, which are being exploited in Tefereyre (75 km northeast of Agadez) by the Nigerian Coal Society (Sonichar) to generate electricity for cities such as Tchirozerin, Agadez, and surrounding towns. Sonichar, founded in 1975, operates a power plant equipped with two thermal units, each generating 18.8 MW. The plant produces approximately 150,000 tonnes of bottom ash (BA) annually, which is currently stored on their premises. In an effort to reduce the substantial amount of mineral waste near their operations and promote positive recycling practices, several feasibility studies have been conducted on the recycling potential of coal bottom ash. Specifically, the focus has been on its use in the manufacturing of novel and environmentally friendly building materials. One area of investigation involves using BA aggregates as secondary granular materials for the production of compressed earth bricks (CEB). CEB technology was selected for this study due to its common usage and suitability in the Sahel region of West Africa. Extensive research has been conducted on CEB technology, including optimization of raw material composition [13], use of natural fibers for reinforcement [14], and analysis of mechanical and thermal properties [15].

Vinai et al. [16] showed that compressed blocks produced with a blend of laterite, BA and Portland cement could achieve average compression strength of 7 MPa, which is higher than the threshold recommended for compressed earth block by CRATerre, i.e., 4-5 MPa [17]. A partial substitution of cement with lime was also investigated in order to ascertain the possibility of reducing the environmental impact deriving from the use of Portland cement. Lawane et al. demonstrated that the compressed blocks made with mixed BA and laterite, along with a blend of Portland cement and lime, could achieve satisfactory strength of about 4 MPa after 90 days of curing [18]. In addition, the laterite, cement and lime-stabilized compressed blocks showed thermal conductivity values in the range of 0.31 to 0.48 W/m·K. Lawane et al. suggested that these results were due to the high porosity of the blocks containing BA (30 to 40%). The inclusion of lateritic soil, Portland cement and lime improved the physical, mechanical and thermal performance of the BA-based blocks [17, 18].

The lateritic soil plays a role in providing cohesion to the grain particles in the production of BA-based blocks. However, excessive use of laterite for the production of stabilized BA-based blocks can lead to environmental problems due to the impact of quarrying

on the landscape. This paper describes the research activities that followed the work of Vinai et al. (2013) and Lawane et al. (2019), focusing on the development and characterization of compressed blocks made with Portland cement-stabilized BA without the inclusion of laterite. The research investigates the use of three different granular classes (i.e., 0/5 mm, 0/2.50 mm, and 0/0.160 mm) of BA and assesses the physical, hydraulic, mechanical, and thermal properties of the developed blocks for their use in the construction sector. The experimental program involves several steps. Firstly, three selected granular classes of BA (0/5 mm, 0/2.5 mm, and 0/0.160 mm) are characterized in terms of chemical composition, specific gravity, and grain size distribution. Subsequently, compressed blocks stabilized with Portland cement only are produced as prisms with dimensions of 14×14×9 cm and 29.5×14×9 cm using a manual Terstaram press. The physical, mechanical, and thermal properties of blocks produced with different BA classes are assessed. The hydric properties, including water-accessible porosity and water absorption, of the blocks are also determined. Finally, the mechanical behavior and fire resistance of BA blocks exposed to temperatures of 200 °C and 400 °C are investigated.

2. Materials and Methods

2.1. Materials.

2.1.1. Bottom ash.

The BA used in this study was sourced from the Sonichar plant in northeastern Niger. The material was collected from the operating site, transported, and prepared in the laboratory following the guidelines of EN 932-2 [19]. Table 1 presents the physical properties and main chemical (oxide) composition of the raw coal BA. To adhere to recommendations for the compressed earth block (CEB) production technique, the BA was screened using a 5 mm sieve, and only particles that passed through this sieve were retained for further study. Additionally, the BA was also screened using a 2.5 mm and 0.160 mm sieve. As a result, three granular classes were selected for the production of the BA-based blocks: fractions of 0/5 mm, 0/2.5 mm, and 0/0.160 mm.

Table 1. Physical and chemical composition (Wt%) of BA [16].

Property	Value
Grain size distribution	Sandy gravels
Specific density	2.2 t/m^3
Bulk density	0.7 t/m^3
Porosity	67%
SiO_2	62.3%
Al_2O_3	27.2%
FeO	3.6%
K_2O	2.6%
TiO_2	2.2%
MgO	0.9%
Na_2O	0.7%
CaO	0.5%
MnO	0.01%

The grain size distribution curves of the three fractions are displayed in Figure 1. Generally, it can be observed that the grain size fractions exhibited narrow range distributions. For the 0-5 mm fraction, approximately 80% of the particles fell within the range of 3 – 5 mm.

On the other hand, the 0-2.5 mm class demonstrated a slightly broader grading, with around 40% of its mass falling within the range of 0.075 – 1.5 mm. The finer class contained approximately 50% of particles smaller than 75 µm, indicating its classification as fine material from a geotechnical perspective.

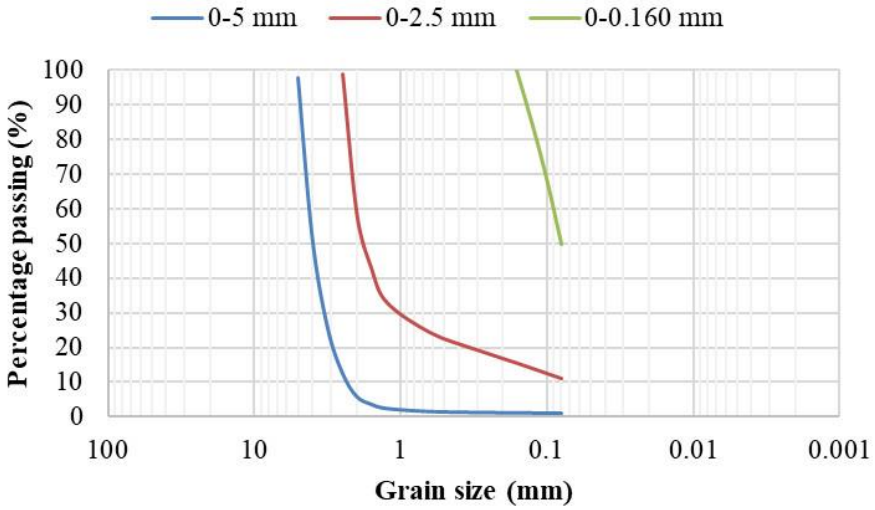

Figure 1. Grain size distribution curves of investigated bottom ash samples.

2.1.2. Portland cement.

The Portland cement utilized in this investigation, namely CPA 45, was provided by Cimtogo, a cement company based in Togo. It conforms to the European cement classification standard EN 197-1 [20] and is classified as CEM I 42.5. Table 2 displays the key properties of the cement used. The cement dosage for stabilization purposes was maintained at 8.5% in volume of the mixture, in accordance with the recommendations of Vinai et al. [16] and Lawane et al. [18].

Table 2. Properties of the cement used in the experiments.

Property	Value
Grain density	3.10 t/m^3
Bulk density	1.06 t/m^3
BET specific Area	1.47 m^2/g
Setting time	180 min

2.2. Methods.

2.2.1. Samples production.

The quantities of constituents were calculated based on volume, as indicated in Table 3. For this investigation, three formulations were chosen corresponding to the grain distributions of BA fractions. The block mixes were labeled as MC5, MC2.50, and MC0.160, representing the granular classes of 5 mm, 2.50 mm, and 0.160 mm, respectively. The BA blocks were manufactured using a Terstaram manual press, which typically applied pressures ranging from 50-60 bar on the material within the mold, occasionally reaching 100 bar. A vertical shaft mixer with a capacity of 100 liters was utilized. The blocks were produced in two sizes: 14 cm x 14 cm x 9 cm (half block) and 29.5 cm x 14 cm x 9 cm (full block). Half block samples were subjected to tests for unconfined compressive strength, thermal properties, hydric behavior,

and fire resistance. Full block samples, on the other hand, underwent three-point bending tests (Fig. 2). Following production, the blocks were covered with a black plastic sheet and slightly moistened for a period of 60 days.

Table 3. Mix proportions of the produced samples.

Label	BA (l)	Cement (l)	Water (l)	Water content of mixing (%)
MC 5	75	7.5	11	16.2
MC 2.50	75	7.5	11	15.6
MC 0.160	75	7.5	11	15.3

Figure 2. BA blocks manufactured.

2.2.2. Physical characterisation.

Specific gravity and thermal properties were assessed for each BA block mix. Specific gravity is the ratio of the grain density $\rho_s$over the water densityρ_w:

$$G_s = \frac{\rho_s}{\rho_w} \quad (1)$$

Grain density was determined using a gas pycnometer in accordance with the ASTM D5550-06 standard. Thermal properties were assessed using the Decagon KD2 PRO equipment [18], which consists of a handheld controller and sensors inserted into the sample. The sensors measure thermal conductivity, resistivity, volumetric specific heat capacity, and diffusivity. Thermal measurements were conducted on samples aged for 28 days.

2.2.3. Hydric characterisation.

Water absorption by capillarity and water-accessible porosity were evaluated for each mix. The coefficient of water absorption by capillarity was determined following the guidelines of ARS 674, 675, 676, and 677. Initially, the samples were dried at a temperature of 40°C until a constant mass was achieved. Subsequently, they were allowed to cool down in open air for 6 hours. The samples were then partially submerged in water with a hydraulic head of 5 mm for a duration of 10 minutes (Fig. 3).

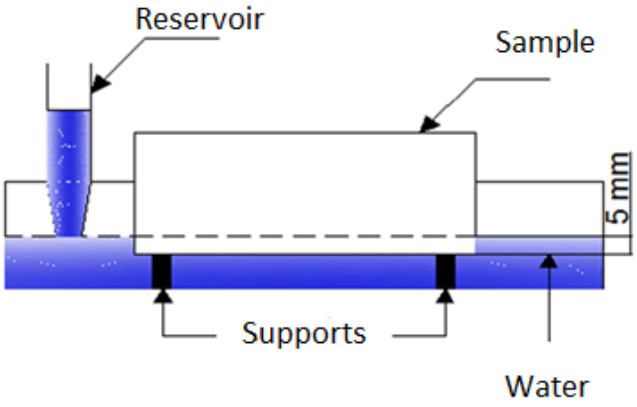

Figure 3. Capillary rise test.

The capillarity absorption coefficient is obtained through the following expression:

$$C = \frac{100\times(m_h - m_s)}{s\sqrt{t}} \quad (2)$$

Where m_h and m_s are the wet and dry masses of blocks respectively (in grams), *s* is the surface of the block immersed in water expressed in cm^2 and t is the immersion time in minutes. The water-accessible porosity was determined in accordance with EN ISO 6275. Samples were initially saturated by immersion in water, then weighted for the determination of their mass in water (m_{eau}). Saturated samples were then weighted in air (m_{air}), then dried in the oven at 105°C (m_{sec}). The porosity ε was determined according to the formula (3):

$$\varepsilon = \frac{m_{air} - m_{sec}}{m_{air} - m_{eau}} \times 100 \quad (3)$$

Results for the capillarity rise and porosity measurements are provided in Section 3.2 and in Figure 5.

2.2.4. Mechanical characterisation

The compressive strength of CEB was determined following the recommendations found in the literature [21]. The tests were conducted using a 1500 kN hydraulic press. An automated data acquisition system was employed, which consisted of an LVDT type displacement sensor with a maximum length of 65 mm and a pressure sensor with a capacity of 400 bar, both connected to the press. Compressive strength measurements were carried out at 28 days of curing, following the guidelines of NF EN 772–1 [22], with six blocks tested for each mix. Additionally, the flexural strength was assessed using a three-point bending test on 29.5 x 14 x 9 cm prisms, and it was calculated using the following formula:

$$R_f = \frac{3\,F\,l}{2\,BH^2} \quad (4)$$

Where *F* is the force at failure, *l*, *B* and *H* are the length, the height and the width of the prism respectively.

Fire resistance tests were conducted on samples that were cured for 28 days. The tests followed the procedure suggested for concrete, as described below [23] and reported by Lawane et al. [18]. The blocks underwent heating-cooling cycles in a furnace, following

specific heating/cooling profiles. The temperature was gradually increased at a rate of 0.5 °C/min until reaching the desired temperature (first phase). Once the desired temperature was reached, the furnace maintained a constant temperature for approximately an hour to ensure uniform heat distribution within each block (second phase). Subsequently, the temperature was gradually decreased at an average rate of 0.5 °C/min until reaching room temperature (third phase). To monitor the temperature on the sides of the bricks during the test, thermocouples were attached. At the end of the third phase, the mass loss and residual compressive strength were measured. Two furnace temperature levels were investigated: 200 °C and 400 °C. These temperatures were selected for comparison with previous studies on blocks of bottom ash with laterite reported in the literature [18]. In total, fifteen samples were tested, including five control samples tested at room temperature (30 °C). The compressive strength of blocks exposed to high temperatures was assessed using a hydraulic press in accordance with the standard NF EN 772–1. Furthermore, ultrasonic pulse velocity (UPV) tests were conducted on the CEB at room temperature (30 °C), as well as on the blocks after exposure to the selected temperatures (200 °C and 400 °C). The purpose of these tests was to evaluate the physical integrity of the blocks after exposure to high temperatures. The ultrasonic pulse velocity in the blocks was measured using the Pundit Plus equipment.

3. Results and Discussion

3.1. Thermo-physical characterisation.

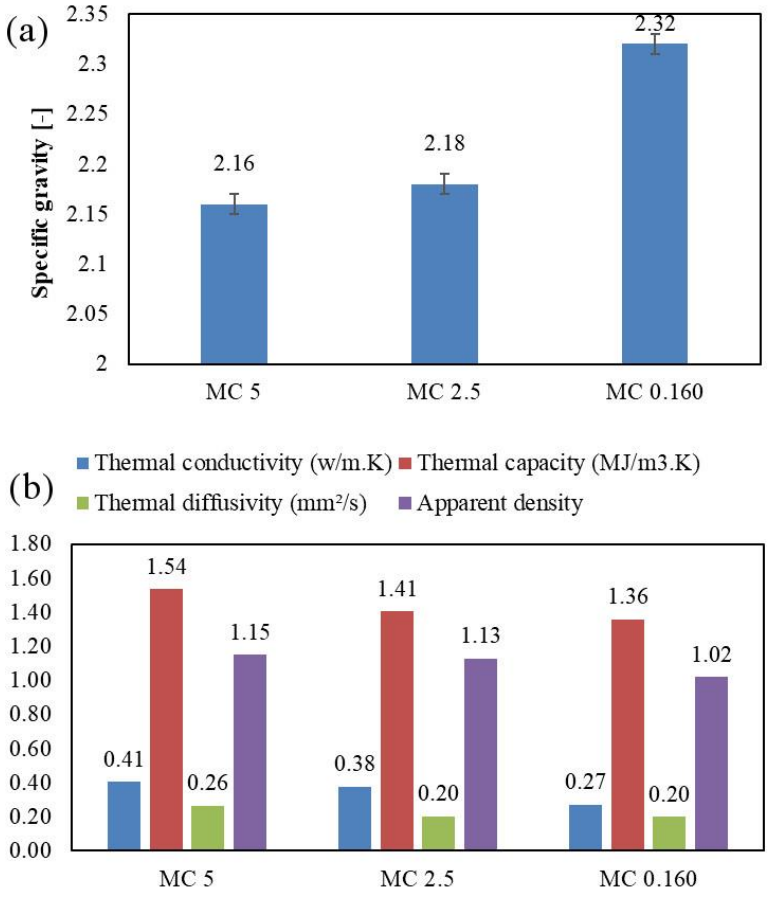

Figure 4. (a) Specific gravity of investigated blocks. (b) Thermo-physical properties of BA blocks.

The specific gravity of the CEB was measured and is shown in Figure 4(a). In general, it was observed that the specific gravity increased as the BA fraction became finer. The specific gravity values obtained in this investigation are comparable to the results reported in the literature (ranging from 1.8 to 2.2) [24]. The results of thermal tests conducted on the CEBs are presented in Figure 4(b). It was noticed that the thermal conductivity values tended to decrease with the granular class of BA, with values ranging from 0.41 to 0.27 W/m·K as the blocks transitioned from MC5 to MC0.160. This result is likely correlated with the decrease in the apparent dry density of the blocks produced using finer BA. The thermal conductivity values obtained for the blocks were lower than those of typical building materials (ranging from 0.70 to 1.30 W/m·K) and lower than those of compressed earth blocks and blocks containing laterite (approximately 0.50 W/m·K), as shown in Table 4. This outcome may be attributed to the lower density of laterite-free CEB (approximately 1.1 g/cm^3) compared to blocks containing laterite (ranging from 1.40 to 1.50 g/cm^3) [18]. Several studies have demonstrated the correlation between the thermal conductivity of blocks and their bulk density [21–27].

Table 4. Thermal conductivity of standard building materials.

Material	Thermal conductivity (W/m.K)	Reference
Mortar	1.40	[25]
Clayey or silty soil	1.50	[25]
Solid concrete	1.15 –2.00	[25]
Hollow concrete blocks	0.70	[26]
Bricks containing lateritic soil with 8% cement	0.75 – 1.15	[26]
Bricks with 45% lateritic soil, 45% natural pozzolana, 10% cement	0.65 –0.71	[26]
Bricks with 81% lateritic soil, 9% sawdust, 10% cement	0.50 –0.65	[28]
Bricks containing laterite with 3 press strokes (28d)	0.56	[28]
Bricks containing laterite with 6 press strokes (28d)	0.61	[28]
Bricks containing laterite with 3 press strokes, 7% lime (28d)	0.86	[28]
Bricks containing laterite with 6 press strokes, 7% lime (28d)	1.00	[28]
Bricks containing laterite with 3 press strokes, 7% lime, 1.4% fibres (28d)	0.76	[28]
Bricks containing laterite with 6 press strokes, 7% lime, 1.4% fibres (28d)	0.80	[28]
Bricks with 10% cement	0.40	[20]
Bricks with 7% cement , 3% lime	0.34	[20]
Bricks with 5% cement, 5% lime	0.31	[20]

3.2. Hydric characterisation

The results of the capillarity absorption rate on the blocks are presented in Figure 5(a). The findings indicate that the capillarity absorption rate decreases as the granular class of BA becomes smaller. Samples MC 5 may have a denser structure and smaller pores compared to samples MC 2.5 and MC 0.160, possibly due to the more heterogeneous range of BA particle sizes. The size of voids within the bricks played a significant role in determining the amount of water absorbed by the surface in contact with water. Smaller voids led to higher capillarity absorption. The porosity accessible to water, as shown in Figure 5(b), appeared to be higher in samples produced with a finer fraction of BA. These results suggested that blocks manufactured with finer BA fractions had higher porosity and relatively larger voids. This could be attributed to the particle size distribution of the finer BA, where the homogeneity of particle sizes resulted in the absence of smaller elements that would fill the voids left by larger elements, leading to higher porosity with relatively larger voids. However, further investigation focused on the size and distribution of pores is necessary to confirm this hypothesis. The presence of cement and the interaction between cement void filling and particle size could also have influenced the measurements of open porosity [29]. The obtained results were generally

consistent with other studies in the literature, which reported water absorption in the range of 35% to 37% for earth mortar with cement dosages exceeding 4% to 5% [29].

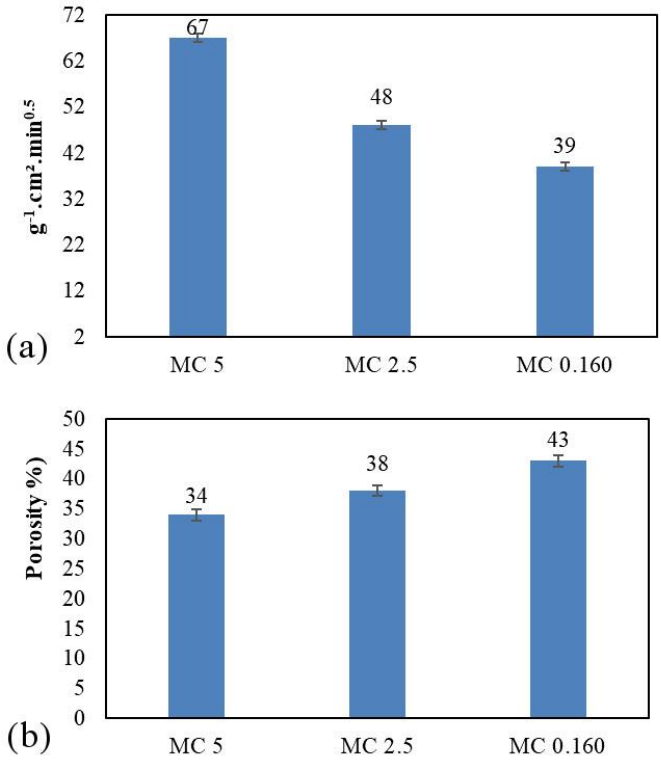

Figure 5. (a) Capillary rise test results; (b) Porosity measured by immersion on samples.

3.3. Mechanical characterisation.

The uniaxial compressive strength of the bricks is depicted in Figure 6(a). It can be observed that the strength results fall within the range of 5 MPa, which is above the threshold recommended by CRATerre (4 MPa) [17], and are consistent regardless of the granular class used for block production. At 28 days of age, the compressive strengths are higher than those reported by Lawane et al. (2019) for BA bricks stabilized with laterite, cement, and lime [18]. The values obtained in this investigation are also higher than those of bricks with laterite produced with 3 press strokes (L/3) and 6 press strokes (L/6) as reported by Toguyeni et al. (2018) [28]. However, the different amount of Portland cement used in the current investigation might explain the higher strengths obtained. The compressive strengths of the blocks in this study are slightly lower than those of other formulations of bricks with laterite produced with 3 or 6 press strokes and stabilized with 7% lime and 1.4% fibers (ranging from 6.05 to 7.19 MPa) [28], suggesting that comparisons among different formulations should be approached with caution. The results are also broadly consistent with the work discussed by Ammari et al. [30], who indicated a compressive strength of about 5 MPa for compressed soil with 52% sand and 13% cement content. However, the effects of different grain size distributions in the present study were less obvious. It could be hypothesized that the better grading observed for the BA class 0-2.5mm (as seen in the grain size distribution curves in Figure 1) might have contributed to a stiffer structure of the blocks. However, the overlap of the error bars, reflecting the standard deviation of the results (as shown in Figure 6(a)), does not allow for a conclusive outcome on this aspect. The results of the three-point bending tests are summarized in Figure 6(b). No significant difference was found among the different formulations. Similar considerations on

the effect of grain size distribution on the strength of the samples (i.e., higher performance of better-graded samples MC 2.5 and MC 0.160) could be made, but the dispersion of the results suggests an overall equivalence among the tested grain size distributions. Nevertheless, a slight increase in flexural strength was observed when the granular class of particles was reduced from 0/5 mm to 0/0.160 mm (or even 0/2.50 mm). It is worth noting that these values remain well above the values of flexural strength (ranging from 0.26 to 0.94 MPa) reported by Toguyeni et al. (2018) [28].

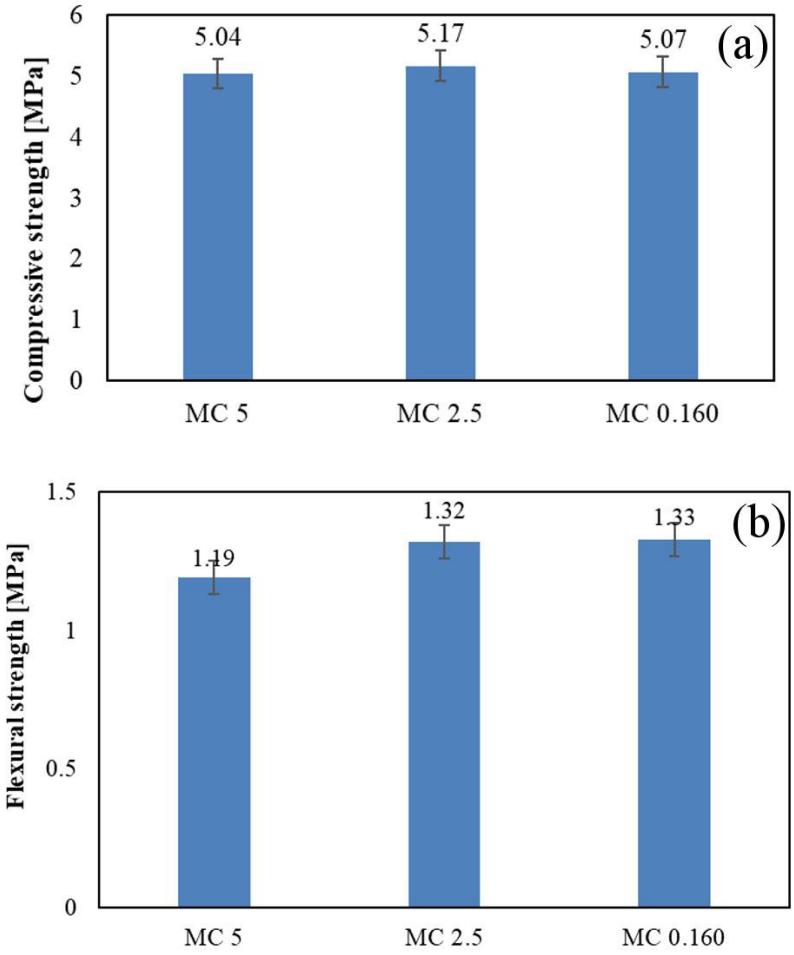

Figure 6. (a) Compressive strength results; (b) Flexural strength results.

The opportunity to test designed grain size distributions obtained by blending different BA classes at different proportions is mentioned in the conclusions section. The results from the fire resistance tests are shown in Figure 7(a). It can be observed that after heating to 200°C, the compressive strength increased by approximately 8% for samples MC 5 and MC 2.5, while it increased by 34% for samples MC 0.160 compared to room temperature. Heating may have led to further chemical reactions involving silicate and aluminate of BA particles, such as the production of amorphous silicoaluminate gel via geopolymerization, which does not depend on cement hydration. The more pronounced increase in strength for samples MC 0.160 can be explained by the specific surface area of the BA grains, which is much higher and thus more prone to reaction. The production of chemical reactions due to the heating process is faster on particles with a high specific surface area compared to those with a lower one. However, microstructural investigations should be carried out to analyze possible reaction products and confirm this hypothesis.

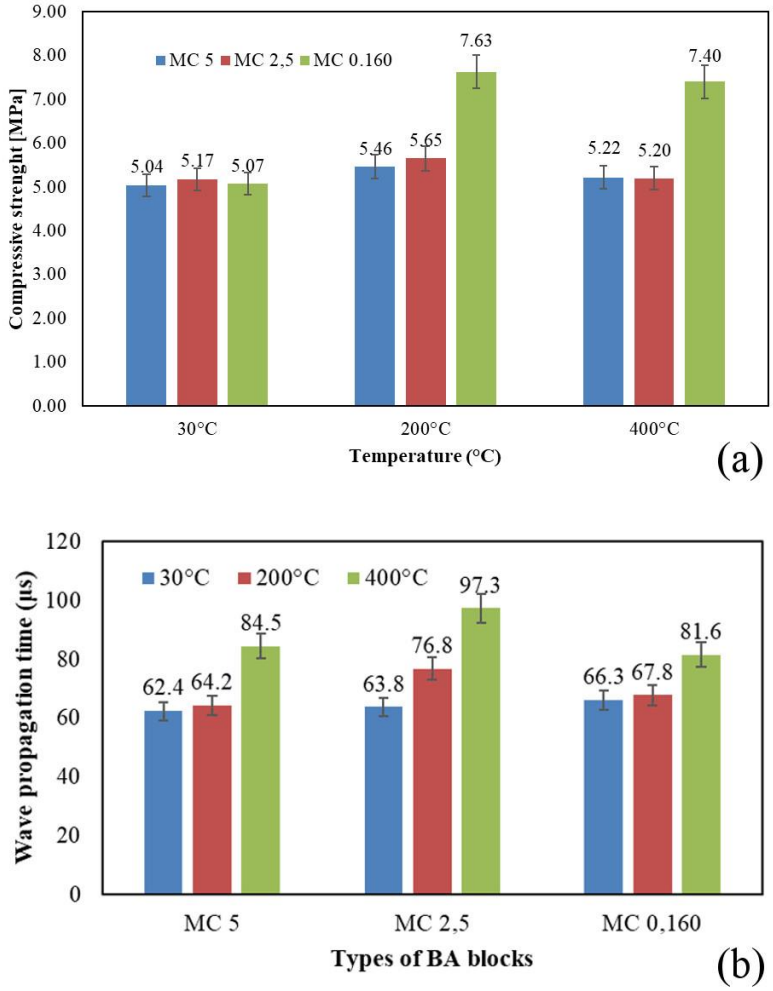

Figure 7. (a) Compressive strength of blocks at ambient temperature and exposed to heating temperature 200°C and 400°C; (b) Ultrasound pulse velocity results at different heating temperatures.

Furnace tests conducted by Lawane et al. (2019) on BA blocks stabilized with Portland cement and laterite resulted in strengths at 200°C higher than the results from the MC 5 sample in this study. This can be explained by assuming that a non-negligible strength contribution was provided by the laterite silicoaluminate content, which, when heated to 200°C, may have led to other Si-Al reaction products, providing an additional gain in resistance to the BA blocks. After heating at 400°C, the mechanical strengths were higher than those obtained at room temperature (30°C). However, a slight reduction in strength compared to the strengths at 200°C was observed. The strength decrease could be explained by considering the onset of thermal decomposition of the C-S-H gel formed from cement hydration, which would weaken the mechanical properties of the bonding matrix. Further heating (e.g., up to 600°C) would be necessary to confirm this hypothesis, along with microstructural characterization such as thermal gravimetric analysis (TGA). No change in the color of the blocks was observed at 200°C or 400°C, confirming the absence of minerals prone to thermal transformation. BA was produced at a high temperature in a coal-fueled thermal power plant, and therefore, no physical or mineralogical variation was expected. No macroscopic cracks were observed on the BA blocks in this experiment. The results from the UPV tests on the BA blocks at different temperatures are shown in Figure 7(b). According to these results, it appears that the wave propagation time increased for samples exposed to 400°C compared to the samples kept at

room temperature (30°C), while the results for samples exposed to 200°C are comparable to the unexposed samples. This result can be explained by assuming that the exposure to 400°C created damages inside the cement matrix (e.g., micro-cracks) and, consequently, increased the travel time of the wavelength within the blocks. On the other hand, exposure to 200°C seemed to have less impact, at least for samples MC 5 and MC 0.160. Further microstructural analyses are needed to confirm these results. The existence of an empirical relationship between compressive strength results and UPV measurements was investigated; however, the data seemed scattered, and no robust numerical correlation could be obtained for the overall dataset as well as for disaggregated results. Further investigation on this aspect could provide useful monitoring tools for the non-destructive testing of CEB wall assemblies.

4. Conclusions

This study investigated the effect of BA size on the physical and mechanical properties of compressed blocks manufactured with coal bottom ash stabilized with Portland cement. Three grain sizes were used for the production of compressed blocks, and a series of physical and mechanical tests were undertaken. The use of finer BA (MC0.160) resulted in lighter blocks with a density of about 1.02 mg/m^3 compared to samples produced with coarser BA (MC5 and MC2.5), presumably due to higher porosity resulting from a more homogeneous grain size distribution. The lower the density, the lower the thermal conductivity, with lambda values in the range of 0.27–0.41 W/m·K, lower than most common building materials. The pore structure of blocks produced with finer BA resulted in lower capillarity absorption compared to samples produced with the 0-5mm fraction, presumably due to a larger void network. Compressive and flexural strengths were approximately 5 MPa and 1.2–1.3 MPa, respectively. The BA size did not seem to significantly affect the value of the mechanical strength. The exposure of blocks to temperatures of 200°C and 400°C did not negatively affect their strength; instead, a strength increase was recorded. Compressive strength exceeded 7 MPa for MC0.160 samples, suggesting that reactions, presumably due to the dissolution and re-condensation of silicate and aluminate species from BA, are fostered by high temperatures, notably in samples with smaller particles having a higher specific surface area. No significant strength reduction or degradation of UPV values was observed after exposure to 200°C. BA blocks can offer better thermal insulation properties than typical building materials and can provide acceptable mechanical strength. Further research should focus on microstructural analysis to confirm the nature of the chemical reactions and the nature and morphology of the pore network. Additionally, further investigation would require the study of blended BA size proportioning and its effects on the mechanical and physical properties of the blocks.

Acknowledgments

Authors would like to thank Sonichar for its financial and technical supports, and wish to express their gratitude to the anonymous reviewers for their contribution in improving the manuscript.

Competing Interest

The authors declare that they have no known competing financial interests or personal relationships that could have appeared to influence the work reported in this paper.

References

[1] What A Waster 2.0. (accessed on 2 December 2021) Available online: http://datatopics.worldbank.org/what-a-waste/.

[2] Park, W.J.; Kim, R,; Roh, S.; Ban, H. (2020). Identifying the Major Construction Wastes in the Building Construction Phase Based on Life Cycle Assessments. *Sustainability, 12*, 8096. https://doi.org/10.3390/su12198096.

[3] Coal Fact. (accessed on 2 April 2020) Available online: https://www.worldcoal.org/coal-facts/.

[4] Le Quéré, C,; Andrew, R.M.; Friedlingstein, P.; Sitch, S.; Pongratz. J.; Manning. A.C.; Korsbakken, J.I.; Peters, G.P.; Canadell, J.G.; Jackson, R.B.; Boden, T.A., et al. (2018). Global Carbon Budget 2017. *Earth System Science Data, 10,* 405–448, https://doi.org/10.5194/essd-10-405-2018.

[5] Asokan, P.; Saxena, M.; Asolekar, S.R. (2005). Coal combustion residues—environmental implications and recycling potentials. *Resources, Conservation & Recycling, 43*, 239–262. https://doi.org/10.1016/j.resconrec.2004.06.003.

[6] Meij, R.; Kokmeijer, E.; Tamboer, L.; Winkel, H.T. (2001). Field leaching of bricks and concrete containing coal fly ash. In International ash utilisation symposium. *Center for Applied Energy Research, 197*, 22–24.

[7] Lemeshev, V.G., Gubin, I.K., Savel'ev, Yu. A., Tumanov, D.V., Lemeshev, D.O. (2004). Utilization of coal-mining waste in the production of building ceramic materials. *Glass and Ceramics, 61*, 9–10. https://doi.org/10.1023/B:GLAC.0000048698.58664.97.

[8] Ravina, D. (1997). Properties of fresh concrete incorporating a high volume of fly ash as partial fine sand replacement. *Materials and Structures & Matériaux et Constructions, 30,* 473–479. https://doi.org/10.1007/BF02524775.

[9] Haibin, L.; Zhenling, L. (2010). Recycling utilization patterns of coal mining waste in China. *Resource Conservation Recycling, 54*, 1331–1340. https://doi.org/10.1016/j.resconrec.2010.05.005.

[10] Baite, E.; Messan, A.; Hannawi, K.; Tsobnang, F.; Prince, W. (2016). Physical and transfer properties of mortar containing coal bottom ash aggregates from Tefereyre (Niger). *Construction and Building Materials, 125*, 919–926. https://doi.org/10.1016/j.conbuildmat.2016.08.117.

[11] Savadogo, N.; Messan, A.; Hannawi, K.; Tsobnang, F.; Agbodjan, W.P. (2015). Durability of composite cement with Tefereyre (NIGER) coal bottom ash: Capillary absorption, porosity to water and acid attack. *Journal of Materials and Engineering Structures 2*, 213–223.

[12] Turco, C.; Junior, A.C.P.; Teixeira, E.R.; Mateus, R. (2021). Optimisation of Compressed Earth Blocks (CEBs) using natural origin materials: A systematic literature review. *Construction and Building Materials, 309*, 125140. https://doi.org/10.1016/j.conbuildmat.2021.125140.

[13] Subramanian, G.K.M.; Balasubramanian, M.; Jeya Kumar, A.A., (2022). A review on the mechanical properties of natural fiber reinforced compressed earth blocks. *Journal of Natural Fibers, 19*, 7687–7701. https://doi.org/10.1080/15440478.2021.1958405.

[14] Teixeira, E.R.; Machado, G., Junior, A.D.P.; Guarnier, C.; Fernandes, J.; Silva, S.M.; Mateus, R. (2020). Mechanical and thermal performance characterisation of compressed earth blocks. *Energies, 13*, 2978. https://doi.org/10.3390/en13112978.

[15] Vinai R.; Lawane A.; Minane J.R.; Amadou A. (2013); Coal combustion residues valorisation: research and development on compressed brick production. *Construction and Building Materials, 40*, 1088–1096. https://doi.org/10.1016/j.conbuildmat.2012.11.096.

[16] Rigassi, V.; CRATerre-EAG (1995). Blocks of compressed earth. Vol. I: Production manual. Friedrich Vieweg and Sohn: Braunschweig, Germany.

[17] Lawane, A.; Minane, J.R.; Vinai, R.; Pantet, A. (2019). Mechanical and physical properties of stabilised compressed coal bottom ash blocks with inclusion of lateritic soils in Niger. *Scientific African, 6*, e00198. https://doi.org/10.1016/j.sciaf.2019.e00198.

[18] EN 932-2:1999 - Tests for general properties of aggregates Methods for reducing laboratory samples. (accessed on 2 January 2022) Available online: https://standards.iteh.ai/catalog/standards/cen/cbfacde6-b57d-48d7-ae43-f886f4c5ec2f/en-932-2-1999.

[19] NF IN 197-1 - Cements. Part 1: composition, specificities and compliance criteria for common cements, April, 40. (accessed on 2 January 2022) Available online: https://standards.iteh.ai/catalog/standards/cen/64d327b1-d5ac-45e3-8b04-fafec9e0698e/en-197-1-2011.

[20] Olivier, M.; Mesbah, A.; Morel, J-C.; El Gharbi, Z. (1997). Test method for strength tests on blocks of compressed earth. *Materials and Structures*, *30*, 515–517. https://doi.org/10.1007/BF02486394.

[21] NF EN 772-1 - Methods for testing masonry elements — Part 1: Determining compression resistance. (accessed on 2 January 2022) Available online: https://standards.iteh.ai/catalog/standards/cen/e16d7005-8730-4382-9a9d-4d351d00f981/en-772-1-2011.

[22] NF P 92-701 - Rules of calculation. Method of forecasting by calculating the fire behaviour of French concrete structures (change of status of the DTU, FB 1987 calculation rule). (accessed on 2 January 2022) Available online: https://dokumen.tips/documents/nf-p-92-701.html.

[23] Rogbeck, J.; Knutz, A. (1996). Coal bottom ash as light fill material in construction. *Waste Management*, *16*, 125–128. https://doi.org/10.1016/S0956-053X(96)00035-9.

[24] Catalogue of constructing elements with U value calculation. (accessed on 14 may 2018) Available online:https://www.fr.ch/sites/default/files/contens/sde/_www/files/pdf67/Catalogue_dlments_de_construction_Construction_neuve_f.pdf.

[25] Meukam, P.; Jannot, Y.; Noumowe, A.; Kofane, T.C. (2004). Thermo physical characteristics of economical building materials, *Construction and Building Materials*, *18*, 437–443. https://doi.org/10.1016/j.conbuildmat.2004.03.010.

[26] Taallah B.; Guettala, A. (2016). The mechanical and physical properties of compressed earth block stabilized with lime and filled with untreated and alkali-treated date palm fibers. *Construction and Building Materials*, *104*, 52–62. https://doi.org/10.1016/j.conbuildmat.2015.12.007.

[27] David, Y.K.; Toguyeni, A.L.; Zoma, F,; Khamis, G. (2018). Formulation of Compressed Earth Blocks Stabilized With Lime and Hibiscus Sabdariffa Fibres Showcasing Good Thermal and Mechanical Properties. *Journal of Materials Science & Surface Engineering, 6*, 817–824.

[28] Ammari, A.; Bouassria, K.; Zakham, N.; Cherraj, M.; Bouabid, H.; D'ouazzane, S.C. (2018). Durability of the earth mortar: Physico-chemical and mineralogical characterization for the reduction of the capillary rise. *MATEC Web of Conferences*, *149*, 01024. https://doi.org/10.1051/matecconf/201714901024.

[29] Ammari, A.; Bouassria, K.; Cherraj, M.; Bouabid, H.; D'ouazzane, S.C. (2017). Combined effect of mineralogy and granular texture on the technico-economic optimum of the adobe and compressed earth blocks. *Case Studies in Construction Materials*, *7*, 240–248. https://doi.org/10.1016/j.cscm.2017.08.004.